UCSF
UC San Francisco Previously Published Works

Title

Use of hyperpolarized [1-13C]pyruvate and [2-13C]pyruvate to probe the effects of the anticancer agent dichloroacetate on mitochondrial metabolism in vivo in the normal rat

Permalink

https://escholarship.org/uc/item/05j0m10n

Journal

Magnetic Resonance Imaging, 30(10)

ISSN

0730-725X

Authors

Hu, Simon
Yoshihara, Hikari AI
Bok, Robert
et al.

Publication Date

2012-12-01

DOI

10.1016/j.mri.2012.05.012

Peer reviewed

eScholarship.org Powered by the California Digital Library
University of California

NIH Public Access
Author Manuscript
Magn Reson Imaging. Author manuscript; available in PMC 2013 December 01.

Published in final edited form as:
Magn Reson Imaging. 2012 December ; 30(10): 1367–1372. doi:10.1016/j.mri.2012.05.012.

Use of Hyperpolarized [1-^{13}C]Pyruvate and [2-^{13}C]Pyruvate to Probe the Effects of the Anticancer Agent Dichloroacetate on Mitochondrial Metabolism *In Vivo* in the Normal Rat

Simon Hu[1], **Hikari A.I. Yoshihara**[1], **Robert Bok**[1], **Jenny Zhou**[2], **Minhua Zhu**[1], **John Kurhanewicz**[1], and **Daniel B. Vigneron**[1]

[1]Department of Radiology and Biomedical Imaging, University of California, San Francisco, CA

[2]School of Medicine, Temple University, Philadelphia, PA

Abstract

Development of hyperpolarized technology utilizing dynamic nuclear polarization has enabled the measurement of ^{13}C metabolism *in vivo* at very high SNR. *In vivo* mitochondrial metabolism can, in principle, be monitored with pyruvate, which is catalyzed to acetyl-CoA via pyruvate dehydrogenase (PDH). The purpose of this work was to determine if the compound sodium dichloroacetate (DCA) could aid the study of mitochondrial metabolism with hyperpolarized pyruvate. DCA stimulates PDH by inhibiting its inhibitor, pyruvate dehydrogenase kinase. In this work, hyperpolarized [1-^{13}C]pyruvate and [2-^{13}C]pyruvate were used to probe mitochondrial metabolism in normal rats. Increased conversion to bicarbonate (+181% ± 69%, p = 0.025) was measured when [1-^{13C}]pyruvate was injected after DCA administration, and increased glutamate (+74% ± 23%, p = 0.004), acetoacetate (+504% ± 281%, p = 0.009), and acetylcarnitine (+377% ± 157%, p = 0.003) were detected when [2-^{13}C]pyruvate was used.

Keywords

Hyperpolarized carbon-13; Dynamic nuclear polarization (DNP); Dichloroacetate (DCA); Pyruvate metabolism; Magnetic resonance spectroscopy

Introduction

Development of hyperpolarized technology utilizing dissolution dynamic nuclear polarization (DNP) has enabled the measurement of ^{13}C metabolism *in vivo* at very high SNR (1). The most widely used DNP agent for both *in vitro* and *in vivo* applications thus far has been [1-^{13}C]pyruvate with its metabolic conversion to [1-^{13}C]lactate and [1-^{13}C]alanine catalyzed by the enzymes lactate dehydrogenase (LDH) and alanine transaminase (ALT) respectively. The levels of these hyperpolarized metabolites have been used to characterize disease state in many preclinical studies. For example, in cancer animal models, dramatic increases in [1-^{13}C]lactate have been detected (2,3,4,5). Deviations in [1-^{13}C]lactate and

© 2012 Elsevier Inc. All rights reserved.

Correspondence to: Dr. Daniel B. Vigneron, Dept. of Radiology and Biomedical Imaging, Box 2512, University of California, San Francisco, 1700 4th St. QB3 Building, Suite 102, San Francisco CA, 94158-2512, Phone: (415) 476-3343, Fax: (415) 514-4451, dan.vigneron@ucsf.edu.

Publisher's Disclaimer: This is a PDF file of an unedited manuscript that has been accepted for publication. As a service to our customers we are providing this early version of the manuscript. The manuscript will undergo copyediting, typesetting, and review of the resulting proof before it is published in its final citable form. Please note that during the production process errors may be discovered which could affect the content, and all legal disclaimers that apply to the journal pertain.

$watermark-text
$watermark-text
$watermark-text

$watermark-text

$watermark-text

$watermark-text

[1-^{13}C]alanine levels (occurring in the cytosol) reflect changes in glycolytic metabolism. Mitochondrial metabolism can also, in principle, be monitored with pyruvate, which is catalyzed to acetyl-CoA via pyruvate dehydrogenase (PDH). In this reaction, the 1-position carbon is oxidized to CO_2 and interconverts to bicarbonate. The 2-position carbon remains on acetyl-CoA, which itself has many possible metabolic fates, including entry into the Krebs cycle, conversion to ketone bodies, lipogenesis, and synthesis of cholesterol and other steroids (6). Figure 1 summarizes these pathways. The purpose of this study was to determine if the compound sodium dichloroacetate (DCA) could aid the study of mitochondrial metabolism with hyperpolarized pyruvate. DCA has the anti-glycolytic effect of stimulating PDH by inhibiting its inhibitor, pyruvate dehydrogenase kinase (PDK) (see Figure 1). In fact, DCA has shown promise as an anticancer agent in numerous *in vitro* studies, preclinical experiments, and most recently, a clinical trial (7,8). By stimulating flux through PDH, DCA is believed to restore mitochondrial function and thereby the apoptotic mechanisms driven by mitochondria (7). The use of DCA has been regarded as a paradigm shift in cancer therapy not only for the approach of targeting tumor metabolism, but also due to DCA being a generic, non-patentable drug that pharmaceutical companies would have no financial interest in (7). Furthermore, the fact that DCA is a small molecule drug that has been safely administered in humans for over 30 years (7) strengthens the rationale to pursue clinical trials despite the lack of industry support (7). In a previous hyperpolarized carbon-13 imaging study, the anti-glycolytic effects of DCA were investigated in NSCLC cells and a mouse tumor model derived from those cells (9). In the current work, hyperpolarized [1-^{13}C]pyruvate and [2-^{13}C]pyruvate were used to probe mitochondrial metabolism in normal rats. Hyperpolarized technology utilizing *both* [1-^{13}C]pyruvate *and* [2-^{13}C]pyruvate is particularly impactful for monitoring response to DCA therapy because it makes possible the direct detection of PDH flux, which is the target of DCA treatment. Metabolic imaging with FDG-PET, as was done in the initial DCA clinical trial (8), does not examine PDH flux directly, but rather upstream uptake of glucose.

Methods

Polarizer and Preparations

All hyperpolarizations were performed using a Hypersense DNP polarizer (Oxford Instruments, Abingdon, UK). For all the experiments, a mixture consisting of 35 μL (approximately 45 mg) of either C_1-labeled or C_2-labeled pyruvic acid (Isotec, Miamisburg, OH, USA) with 15 mM OX063 trityl radical and 1.5 mM Dotarem® gadolinium was polarized. The preparation was polarized for 1 hour and then dissolved and neutralized in an aqueous solution with 40 mM Tris, 100 mM NaOH, and 0.3 mM Na_2EDTA. The final dissolved pyruvate had a concentration of 100mM and a pH of ~7.5. The liquid state polarizations for [1-^{13}C]pyruvate and [2-^{13}C]pyruvate were typically >30% and >27% respectively at the time of dissolution.

Animal Handling

All animal studies were carried out under a protocol approved by the Institutional Animal Care and Use Committee. Normal male Sprague-Dawley rats were used. For each experiment, a rat was anesthetized with an initial dose of isoflurane (2–3%), placed on a heated pad, and had a tail vein catheter inserted while under continuous anesthesia (1–2% isoflurane). An extension tube was attached to the main catheter to facilitate the eventual administration of the hyperpolarized substrate. The rat was then transferred to a heated water pad (37 °C, continuous flow) in the radiofrequency (RF) coil in the MR scanner, strapped in place, kept under anesthesia with continuous delivery of isoflurane (1–2%) through a long tube to a nose cone (oxygen flow of 1 L/min), and periodically monitored. Sodium dichloroacetate (Sigma Aldrich, St. Louis, MO, USA) was dissolved in saline (100 mg/mL)

$watermark-text

$watermark-text

$watermark-text

and administered to each rat. The first dose of DCA (150 mg/kg) was given intraperitoneally right after a baseline carbon-13 imaging experiment, and another dose of DCA (150 mg/kg) was given intravenously 5 minutes before the follow-up carbon-13 imaging experiment.

MR Studies

All experiments were performed on a 3T MR scanner (GE Healthcare, Waukesha, WI, USA) equipped with multinuclear spectroscopy capability. A custom dual-tuned $^{1}H/^{13}C$ rat coil with a quadrature ^{13}C channel and a linear ^{1}H channel was used. The coil design was the same as in (10), and the coil measured 15.25 cm in length with an 8.3 cm inner diameter. Axial T2-weighted anatomical images were acquired with a standard fast spin-echo sequence. For the carbon-13 imaging, non-localized baseline and follow-up scans were conducted 1.5 hours apart. In the [1-^{13}C]pyruvate scans, a double spin-echo sequence with adiabatic refocusing pulses (11) with TE = 35 ms, TR = 3 sec, and 5 degree (500 μsec) hard pulse excitation was used. The 500 μsec 5 degree hard pulse had an amplitude of 0.0065 gauss and required 0.135 mW of power delivered to the rat coil. The adiabatic pulses were 1.7 gauss in amplitude and required 9.2 W of power. 2.5 mL of 100 mM pyruvate was delivered into the animal over 12 seconds (no flush), with data collection starting at the same time as the injection. In the [2-^{13}C]pyruvate scans, the adiabatic pulses (11) in the double spin-echo sequence were removed and the 5 degree hard pulse was shortened to 32 μsec to increase excitation bandwidth. This increased the pulse amplitude and power to 0.102 gauss and 33 mW respectively. (Note that without the adiabatic pulses, the echo could be collected immediately after the excitation, thereby shortening TE to essentially 32 μsec.) In addition, 3 mL of 100 mM [2-^{13}C]pyruvate was injected. Otherwise, all parameters between the [1-^{13}C]pyruvate and [2-^{13}C]pyruvate scans were the same.

Data Analysis

For each dynamic time point, a 10 Hz Gaussian apodization filter was used, a 1D FFT was performed, and a zero-order phase correction was applied. The first 32 time points were summed together, and for metabolite quantification, noise-subtracted area ratios were used. For the quantification of metabolites after injection of [2-^{13}C]pyruvate, a local baseline correction (assuming a linear baseline in that region) was first applied. Paired student t-tests were used for all statistical comparisons.

Results

Figure 2 shows non-localized rat spectra after injection of [1-^{13}C]pyruvate pre and post DCA. The vertical scales are zoomed in about a factor of 6 to highlight the lactate, alanine, and bicarbonate peaks. As expected from stimulation of the PDH pathway, there was a dramatic increase in bicarbonate after DCA administration. A total of n = 4 rats were studied with [1-^{13}C]pyruvate, and the bicarbonate/pyruvate ratio (where pyruvate is the sum of pyruvate and pyruvate-hydrate) increased by 181% ± 69% (mean ± standard deviation) with p = 0.025, providing evidence that the DCA was indeed effective in increasing the *in vivo* PDH enzymatic conversion of pyruvate to acetyl-CoA. The (lactate + alanine)/pyruvate ratios were also quantified with only a minor but not statistically significant reduction observed (−5.7% ± 16.6%, p = 0.63). Figure 3 shows and lists the peaks detected in a non-localized spectrum after DCA administration and injection of [2- ^{13} C]pyruvate. The chemical shift values in Figure 3 are referenced to the injected [2-^{13}C]pyruvate at 207.8 ppm. Peaks were assigned by consulting a standard metabolome database (http://www.hmdb.ca/), considering plausible metabolic pathways, and comparing with results from a prior study using hyperpolarized [2-^{13}C]pyruvate (12). All of the chemical shifts for the metabolite peaks in Figure 3 matched closely with those from (12) except that the acetoacetate peaks were not detected in (12). This was not surprising given that the authors

$watermark-text

$watermark-text

$watermark-text

in (12) did not stimulate the PDH pathway, and in this study we observed the acetoacetate peaks reliably (Figure 4) only after DCA administration. Most of the signal came from the injected [2-^{13}C]pyruvate and its equilibrium partner [2-^{13}C]pyruvate-hydrate, but appreciable metabolic products could also be detected. In particular, the highlighted box in Figure 3 shows a group of metabolite signals ([5-^{13}C]glutamate, [1-^{13}C]acetoacetate, [1-^{13}C]acetylcarnitine, and [1,2-$^{13}C_2$]pyruvate) on which quantitation was performed. Figure 4 shows the pre and post DCA spectra zoomed in on glutamate, acetoacetate, acetylcarnitine, and pyruvate. As shown in Figure 4, glutamate increased modestly relative to pyruvate, and acetoacetate and acetylcarnitine increased dramatically. For quantification purposes, the area of the right peak in the pyruvate doublet was used. Across n = 4 rats, the glutamate/pyruvate ratio increased by 74% ± 23% ($p = 0.004$), the acetoacetate/pyruvate ratio increased by 504% ± 281% ($p = 0.009$), and the acetylcarnitine/pyruvate ratio increased by 377% ± 157% ($p = 0.003$). As shown in Figure 3, there was some residual baseline after zero-order phasing of the spectrum. This baseline was locally corrected in the region highlighted in Figure 3 before quantitation of the metabolites shown in Figure 4.

Discussion

In this study, it was demonstrated that sodium dichloroacetate could be used to enhance flux through the PDH pathway and thus aid the investigation of mitochondrial metabolism using hyperpolarized carbon-13 substrates. The increase in ^{13}C-bicarbonate (in equilibrium with $^{13}CO_2$, which comes directly from [1-^{13}C]pyruvate entering the mitochondria) strongly indicates that DCA was effective in stimulating pyruvate flux through PDH. Acetyl-CoA derived from pyruvate entering the mitochondria has several possible metabolic fates. One of those is entry into the Krebs cycle, which was indicated by the detection of glutamate, as shown in Figure 4. Another fate is attachment to carnitine via carnitine acyltransferase I to form acetylcarnitine. As suggested by Figure 4, at least in the normal rat, much of the excess acetyl-CoA goes to form acetylcarnitine. In addition, acetyl-CoA can be converted to ketone bodies, and accordingly, Figure 4 demonstrates production of the ketone body acetoacetate. Other metabolic fates, such as lipid synthesis, are probably not detectable with hyperpolarized ^{13}C due to binding with large enzymes that cause rapid spin-lattice relaxation.

The results from this study show that changes in carnitine metabolism were detected in response to a physiological perturbation. A substantial portion of the excess acetyl-CoA was shunted to acetylcarnitine, essentially labeling the carnitine pool. Carnitine is synthesized in the liver, kidneys, and brain and is crucial in the transport of fatty acids to mitochondria for oxidation in muscle and cardiac tissue (13). It has been administered as a neuroprotective agent and in disorders that involve carnitine deficiency. Such a deficiency is present in diabetes, cirrhosis of the liver, and other metabolic disorders. In the liver, carnitine deficiency has been linked to excessive lipid accumulation (13). Thus, acetylcarnitine could be a potential biomarker for disruption of metabolism in liver disease.

The excess acetyl-CoA was also directed to form ketone bodies, such as acetoacetate. Ketogenesis occurs in the liver to produce and export fuel for extrahepatic tissues. Ketone bodies are overproduced during starvation and diabetes and can lead to acidosis (14). Normal liver only produces and does not consume acetoacetate, but elevated activity of acetoacetyl-CoA transferase, involved in the catabolism of acetoacetate, has been detected in a rat liver cancer model (14). Therefore, it is possible that diseased liver will exhibit hyperpolarized acetoacetate levels that differ from healthy liver, making it a potential biomarker as well. In addition, hyperpolarized acetate itself may also be a good agent for liver cancer studies, as [^{11}C]acetate is being investigated as a PET tracer for cancer (14).

$watermark-text

$watermark-text

$watermark-text

Detecting the metabolic products listed above (from both [1-^{13}C]pyruvate and [2-^{13}C]pyruvate) and thus monitoring flux through PDH would, of course, also have utility if DCA were used as a cancer therapy (7, 8). Hyperpolarized technology would have the distinct advantage over other metabolic imaging modalities of being able to specifically monitor the PDH pathway, which is targeted by DCA. The strong signal to noise ratio made possible by hyperpolarized technology means that localized imaging may be possible for future preclinical and clinical studies involving DCA, DCA analogs, and other PDK inhibitors (15). Overall, the specificity of hyperpolarized technology to monitor PDH flux could assist in drug development and targeted imaging of this pathway in patients.

Hyperpolarized ^{13}C metabolic imaging has distinct advantages, such as high sensitivity, virtually no background signal, and no ionizing radiation. It has the potential to become clinically applicable (16), and use of hyperpolarized ^{13}C technology to track metabolism could substantially impact the diagnosis, staging, and measurement of response to therapy of disease (16). Much attention has already been given to the use of [1- ^{13}C]pyruvate in preclinical cancer models, where it has been shown that perturbation of glycolysis in tumors results in elevated hyperpolarized [1-^{13}C]lactate levels (2, 3, 4, 5). The utility of hyperpolarized technology, though, extends beyond probing glycolysis. At least in preclinical applications, it is feasible to study mitochondrial metabolism using [2-^{13}C]pyruvate, as shown in this work. The use of DCA and hyperpolarized [2-^{13}C]pyruvate would also be appropriate in cell culture studies. In these scenarios, DNP technology is especially beneficial in that investigations of steady state levels of low concentration metabolites would be severely limited without the sensitivity enhancement from hyperpolarization. In the current study, DCA was used to modulate the PDH pathway, and a change was detected using hyperpolarized ^{13}C MR. Changes in the PDH pathway are also associated with the actions of a single oncogene, such as MYC in the liver (5), another reason [2-^{13}C]pyruvate may be of interest as an agent for future cancer studies. The observations in the normal rat in the current study could serve as the basis for future disease studies. The continued investigation of agents beyond [1-^{13}C]pyruvate in animal models could lead to new biologically-relevant hyperpolarized biomarkers and promote the development of novel metabolic imaging approaches useful for the individualized treatment of disease.

Conclusions

Metabolic changes were detected *in vivo* in normal rats in response to a physiological perturbation in the pyruvate dehydrogenase pathway, namely stimulation with the compound DCA. Increased production of acetyl-CoA from pyruvate occurred, as detected by increased glutamate, acetoacetate, and acetylcarnitine. These results in normal rats may provide the basis for future disease studies.

Acknowledgments

The authors thank Dr. James Tropp for designing and building the coil used in this study. This study was supported by NIH grants R01EB007588 and P41EB013598.

References

1. Ardenkjaer-Larsen JH, Fridlund B, Gram A, Hansson G, Hansson L, Lerche MH, Servin R, Thaning M, Golman K. Increase in signal-to-noise ratio of > 10,000 times in liquid-state NMR. Proc Natl Acad Sci. 2003; 100:10158–10163. [PubMed: 12930897]

2. Golman K, Zandt RI, Lerche M, Pehrson R, Ardenkjaer-Larsen JH. Metabolic imaging by hyperpolarized ^{13}C magnetic resonance imaging for *in vivo* tumor diagnosis. Cancer Res. 2006; 66:10855–10860. [PubMed: 17108122]

$watermark-text
$watermark-text
$watermark-text

3. Day SE, Kettunen MI, Gallagher FA, Hu DE, Lerche M, Wolber J, Golman K, Ardenkjaer-Larsen JH, Brindle KM. Detecting tumor response to treatment using hyperpolarized ^{13}C magnetic resonance imaging and spectroscopy. Nat Med. 2007; 13:1382–1387. [PubMed: 17965722]
4. Albers MJ, Bok R, Chen AP, Cunningham CH, Zierhut ML, Zhang V, Kohler SJ, Tropp J, Hurd RE, Yen Y, Nelson SJ, Vigneron DB, Kurhanewicz J. Hyperpolarized ^{13}C lactate, pyruvate, and alanine: noninvasive biomarkers for prostate cancer detection and grading. Cancer Res. 2008; 68:8607–8615. [PubMed: 18922937]
5. Hu S, Balakrishnan A, Bok RA, Anderton B, Larson PEZ, Nelson SJ, Kurhanewicz J, Vigneron DB, Goga A. ^{13}C-Pyruvate imaging reveals alterations in glycolysis that precede tumor formation and regression. Cell Metab. 2011; 14:131–142. [PubMed: 21723511]
6. Nelson, DL.; Cox, MM. Lehninger Principles of Biochemistry. 5. New York: W.H. Freeman and Company; 2008.
7. Michelakis ED, Webster L, Mackey JR. Dichloroacetate (DCA) as a potential metabolic-targeting therapy for cancer. Brit J Cancer. 2008; 99:989–994. [PubMed: 18766181]
8. Michelakis ED, Sutendra G, Dromparis P, Webster L, Haromy A, Niven E, Maguire C, Gammer TL, Mackey JR, Fulton D, Abdulkarim B, McMurtry MS, Petruk KC. Metabolic modulation of glioblastoma with dichloroacetate. Sci Transl Med. 2010; 2:31ra34.
9. Seth P, Grant A, Tang J, Vinogradov E, Wang X, Lenkinski R, Sukhatme VP. On-target inhibition of tumor fermentative glycolysis as visualized by hyperpolarized pyruvate. Neoplasia. 2011; 13:60–71. [PubMed: 21245941]
10. Derby K, Tropp J, Hawryszko C. Design and evaluation of a novel dual-tuned resonator for spectroscopic imaging. J Magn Reson. 1990; 86:645–651.
11. Cunningham CH, Chen AP, Albers MJ, Kurhanewicz J, Hurd RE, Yen Y, Pauly JM, Nelson SJ, Vigneron DB. Double spin-echo sequence for rapid spectroscopic imaging of hyperpolarized ^{13}C. J Magn Reson. 2007; 187:357–362. [PubMed: 17562376]
12. Schroeder MA, Atherton HJ, Ball DR, Cole MA, Heather LC, Griffin JL, Clarke K, Radda GK, Tyler DJ. Real-time assessment of Krebs cycle metabolism using hyperpolarized ^{13}C magnetic resonance spectroscopy. FASEB J. 2009; 23:2529–2538. [PubMed: 19329759]
13. Flanagan JL, Simmons PA, Vehige J, Willcox MDP, Garrett Q. Role of carnitine in disease. Nutrition & Metab. 2010; 7:30–43.
14. Leung K. MICAD. 2008
15. Kato M, Li J, Chuang JL, Chuang DT. Distinct structural mechanisms for inhibition of pyruvate dehydrogenase kinase isoforms by AZD7545, dichloroacetate, and radicicol. Structure. 2007; 15:992–1004. [PubMed: 17683942]
16. Kurhanewicz J, Vigneron DB, Brindle K, Chekmenev EY, Comment A, Cunningham CH, Deberardinis RJ, Green GG, Leach MO, Rajan SS, Rizi RR, Ross BD, Warren WS, Malloy CR. Analysis of cancer metabolism by imaging hyperpolarized nuclei: prospects for translation to clinical research. Neoplasia. 2011; 13:81–97. [PubMed: 21403835]

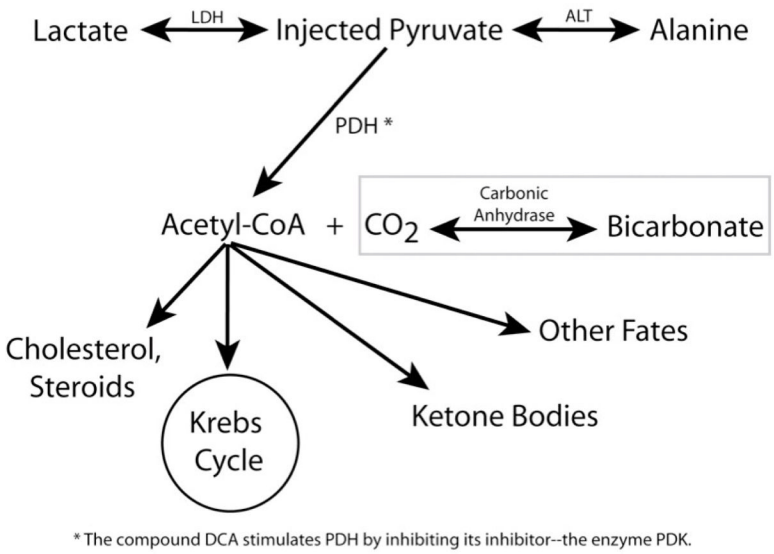

Figure 1.

Summary of key metabolic pathways. The injected pyruvate is converted to lactate and alanine in the cytosol. Pyruvate is irreversibly catalyzed to acetyl-CoA + CO_2 (CO_2 in equilibrium with bicarbonate) in the mitochondria by the enzyme PDH. The compound DCA can be used stimulate PDH by inhibiting its inhibitor—the enzyme PDK. The metabolic fates of acetyl-CoA include entry into the Krebs cycle and formation of ketone bodies.

$watermark-text
$watermark-text
$watermark-text

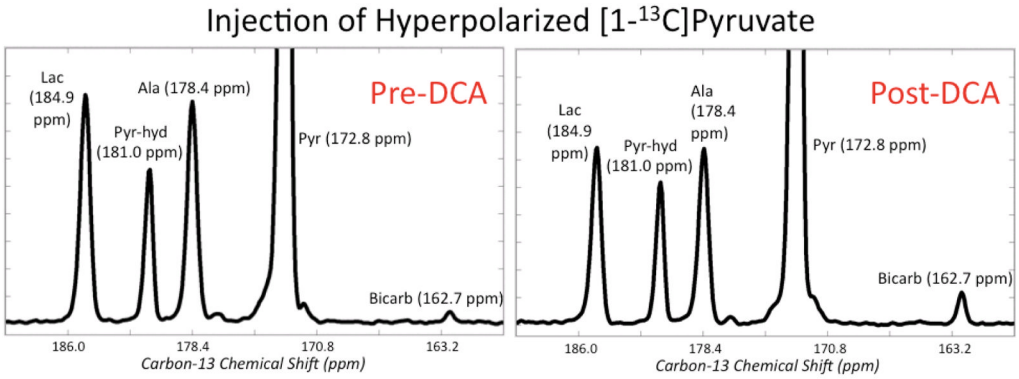

Figure 2.

Representative non-localized rat spectra after injection of [1-^{13}C]pyruvate pre and post DCA. The vertical scales are zoomed in by about a factor of 6 to highlight the lactate, alanine, and bicarbonate peaks. The major difference between the pre-DCA (left) and post-DCA (right) spectra is the dramatic increase in bicarbonate following DCA administration, indicating that DCA was effective in stimulating the PDH pathway.

$watermark-text
$watermark-text
$watermark-text

$watermark-text

$watermark-text

$watermark-text

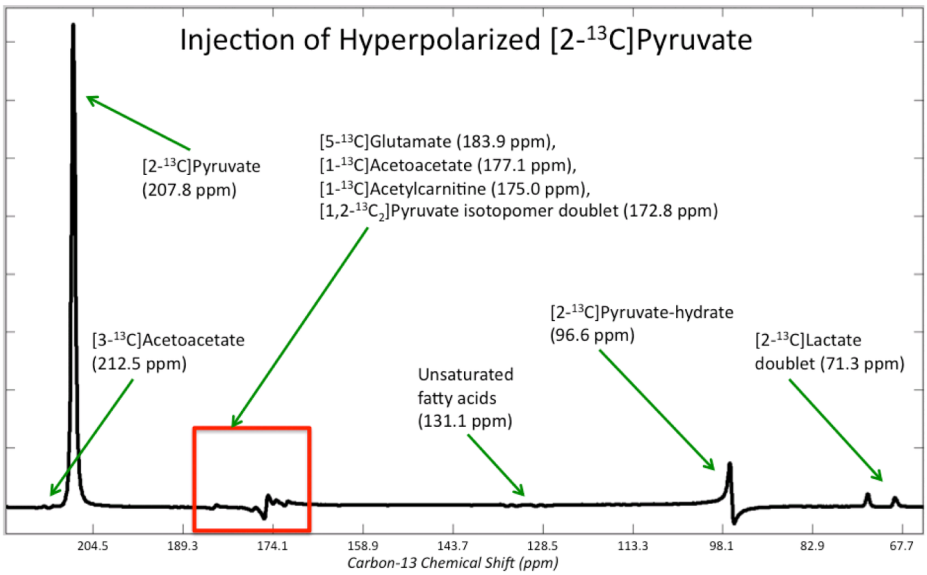

Figure 3.

Representative non-localized spectrum after DCA administration and injection of [2-^{13}C]pyruvate. The peak assignments along with their chemical shifts are shown (ppm values are given with respect to the injected [2-^{13}C]pyruvate's chemical shift of 207.8 ppm). Pyruvate is in equilibrium with pyruvate-hydrate and is enzymatically converted to lactate and acetyl-CoA. Through [1-^{13}C]acetyl-CoA, [5-^{13}C]glutamate, [1-^{13}C]acetoacetate, and [1-^{13}C]acetylcarnitine were produced and detected. Figure 4 shows zoomed in spectra of the highlighted box containing glutamate, acetoacetate, acetylcarnitine, and pyruvate.

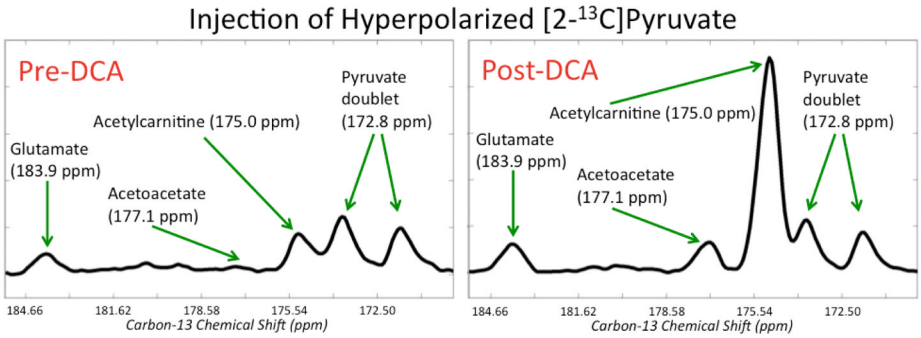

Figure 4.

Representative non-localized rat spectra after injection of [2-^{13}C]pyruvate pre- and post-DCA zoomed in on [5-^{13}C]glutamate, [1-^{13}C]acetoacetate, [1-^{13}C]acetylcarnitine, and [1,2-$^{13}C_2$]pyruvate. This is the highlighted region from Figure 3. Glutamate increased modestly relative to pyruvate, and acetoacetate and acetylcarnitine increased dramatically. Note that in this figure and for subsequent quantitation, local baseline correction was applied.

$watermark-text
$watermark-text
$watermark-text